Ghahfarokhi, Payam Shams; Kallaste, Ants; Vaimann, Toomas; Rassolkin, Anton; Belahcen, Anouar

Steady-state thermal model of a synchronous reluctance motor

Published in:
Proceedings of the 2018 IEEE 59th Annual International Scientific Conference on Power and Electrical Engineering of Riga Technical University, RUTCON 2018

DOI:
10.1109/RTUCON.2018.8659846

Published: 04/03/2019

Document Version
Peer-reviewed accepted author manuscript, also known as Final accepted manuscript or Post-print

Please cite the original version:
Ghahfarokhi, P. S., Kallaste, A., Vaimann, T., Rassolkin, A., & Belahcen, A. (2019). Steady-state thermal model of a synchronous reluctance motor. In *Proceedings of the 2018 IEEE 59th Annual International Scientific Conference on Power and Electrical Engineering of Riga Technical University, RUTCON 2018* Article 8659846 IEEE. https://doi.org/10.1109/RTUCON.2018.8659846

Steady-State Thermal Model of a Synchronous Reluctance Motor

Payam Shams Ghahfarokhi, Ants Kallaste,
Toomas Vaimann, Anton Rassolkin
Dept. Electrical Power Engineering and Mechatronics
Tallinn University of Technology
Tallinn, Estonia
payam.shams@ttu.ee

Anouar Belahcen
Dept. Electrical Power Engineering and Mechatronics
Tallinn University of Technology
Tallinn, Estonia
Dept. of Electrical Engineering and Automation
Aalto University
Finland

***Abstract*— This paper presents an analytical thermal model of a synchronous reluctance motor (SynRMs) to predict the temperature of its different parts. For the analytical calculation, a lumped parameter thermal network (LPTN) is developed and analyzed. To validate the developed model, measurements are carried out on an experimental setup including the analyzed machine. Finally, the test results are compared with the analytical results to assess the accuracy of the model.**

Keywords—ac motors; lumped parameter thermal network;Synchronous reluctance motor; thermal analysis; thermal model

I. INTRODUCTION

Recently, there has been a growing interest in SynRMs due its low cost and simple structure as well as simple construction and manufacturing process [1]. This topology is presented as the right choice for traction and high-speed applications. A number of efforts has been done to achieve higher torque and power density, higher energy efficiency, and cost reduction. To achieve these goals, the thermal analysis of the electrical machine in parallel with the electromagnetic design is necessary.

The thermal analysis of an electrical machine is divided into two categories; analytical LPTN and finite element analysis (FEA) [2],[3]. The FEA has an ability to model complex shapes as well as accurate conduction heat transfer and heat loss distribution inside solid materials [2], [4] However, it is a time-consuming method and the convection boundaries are evaluated by means of the same empirical and analytical correlations which are applied for the LPTN[4], [5].

Some advantages of LPTN compared to the FEA are the fast calculation time with an acceptable accuracy. The thermal designers of electrical machines apply this method to evaluate the temperature of the key components of the electrical machine. There is a number of reports for LPTN analysis of the electrical machines [5]-[10]. Most of these reports deal with LPTN of the induction [6]-[9] and permanent magnet synchronous machines [5],[10]. In some models e.g., the proposed thermal model in [6], the heat transfer paths have been developed in both radial and axial directions. As a result, the network complexity in terms of model details such as the number of nodes and thermal resistances and the calculation time has been increased. In order to tackle the mentioned problems, Boglietti in [9], presented a simplified thermal network for an induction motor. Accordingly, the number of the thermal nodes has been reduced to six and the axial heat transfer paths have been confined to the shaft and the end-windings.

There has been a small number of reports describing the thermal model of the SynRMs. e.g., in [11], Rasid mainly focused on the heat transfer inside the stator slots and proposed a thermal model for the active part of the machine. In [1], Boglietti used the FEA for modeling these active parts of the machine.

This paper presents a simplified LPTN for a SynRM based on the proposed thermal model in [9]. This model has been specially developed for steady-state thermal analysis of a totally enclosed fan cooled (TEFC) transverse- laminated SynRM.

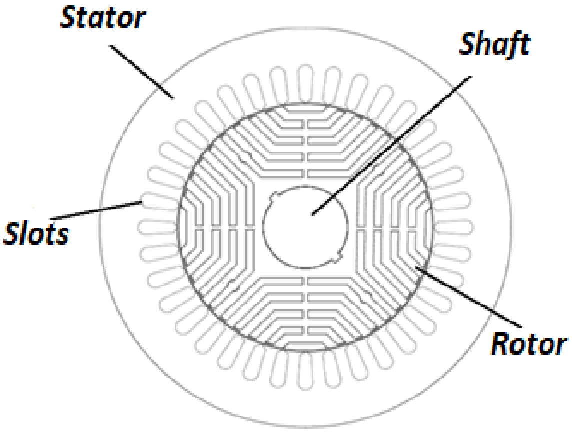

Fig. 1. The cross-section of the 11-kW transverse-laminated SynRM analyzed in this paper.

This work was supported by the Estonian Research Council grant PUT (PUT1260).

II. THERMAL MODEL DETAILS

A. Thermal Model Equivalent Circuit

The thermal model developed in this paper is intended for a four poles 10 kW, 400 V, 50 Hz, transverse-laminated SynRM with F insulation class, which its cross-section is shown in Fig. 1. Table I and II show the geometrical and material data of the experimental SynRM.

TABLE I. GEOMETRICAL DATA OF TRANSVERSE- LAMINATED SYNRM

Name	**Unit**	**Value**
Stator core length	*mm*	156
Stator inner diameter	*mm*	136
Stator outer diameter	*mm*	219
Number of slots	-	36
Air-gap height	*mm*	0.4
Rotor inner diameter	*mm*	45
Rotor outer diameter	*mm*	135.2
Coil height	*mm*	21
Slot filling factor	-	0.6
Slot area	mm^2	130.1

TABLE II. MATERIAL DATA OF TRANSVERSE- LAMINATED SYNRM

Machine part	**Material**	**Thermal conductivity (W/mK)**
Frame	Aluminum	230
Laminations	Electric steel	28
Winding	Copper	387
Impregnation	Resin	0.2
Air gap	Air	0.0257
Shaft	Steel	41

To model the steady-state thermal behavior of the machine with the LPTN method, the different heat transfer paths and thermal losses of the machine are represented by means of impedances and power sources respectively. During this process, we implement some hypotheses to reduce the complexity of the thermal model. E.g., the heat losses distribution is assumed to be uniform, the heat flux can only transfer in the axial direction through the shaft, end-winding and end regions of the machine, the heat flux distribution in both end regions of the machine are analogous.

Figure 2 presents the developed LPTN of the machine. The thermal model consists of five nodes and 13 thermal resistances, which capture all the key thermal parameters and temperature raises as well as the main thermal heat transfer paths. Table III gives the definition of the thermal model components of Fig. 2.

Since the SynRM has the same stator structure as an induction machine, the only difference between the developed thermal model in Fig. 2 with the thermal model of the induction machine proposed in [9] is the rotor model. Precisely, the only thermal resistances which will be different from the proposed model in [9] are R_{10} and R_{11}. The detailed evaluation methods of the other thermal resistances in Table III can be found in [9] and are not described here.

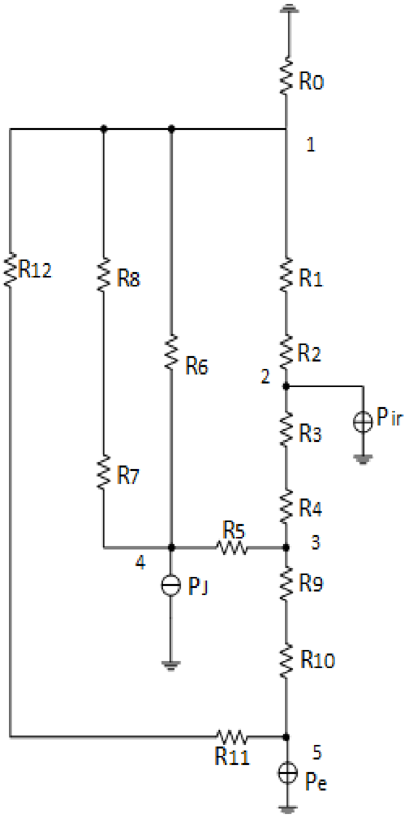

Fig. 2. The developed LPTN model of SynRM.

TABLE III

DEFINITION OF THERMAL MODEL COMPONENTS

Component	**Description**
R_0	Natural Convection and radiation thermal resistance from frame surfer to ambient
R_1	Interface gap conduction thermal resistance between the frame and active part of the machine
R_2	Conduction thermal resistance of the upper half side of the stator yoke
R_3	Conduction thermal resistance of the lower half side of the stator yoke
R_4	Conduction thermal resistance of the stator teeth
R_5	Conduction thermal resistance between the stator winding and stator teeth
R_6	Conduction thermal resistance between the stator winding and frame
R_7	Convection thermal resistances between the stator end-winding and inner air of end region
R_8	Convection thermal resistance between the inner air and end cap
R_9	Convection thermal resistance of the air gap
R_{10}	Conduction thermal resistance of upper half side of the rotor
R_{11}	Conduction thermal resistance the lower half part of the rotor
R_{12}	Axial thermal conduction of the shaft
P_{ir}	Stator iron losses
P_J	Stator joule losses
P_e	Rotor iron losses

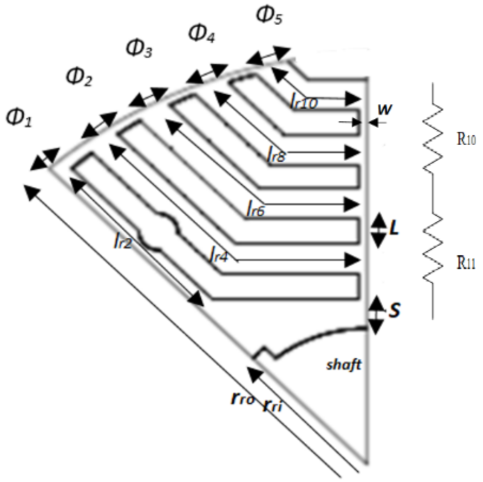

Fig. 3. Cross section of 1/8 of the rotor.

B. Calculation of Rotor Thermal Resistances

Figure 3 shows the geometry of a half a pole of the SynRM rotor. The rotor construction consists of the iron laminations, which makes the magnetic flux paths and air gaps in the laminations, which are the magnetic flux barriers. By using the hypothesis that the heat transfer inside the flux barriers is carried out through natural convection and also due to the high thermal conductivity of the rotor iron laminations; we eliminate the heat transfer by the natural convection phenomenon from magnetic flux barriers. As a result, the total heat fluxes inside the rotor are transferred from the iron laminations.

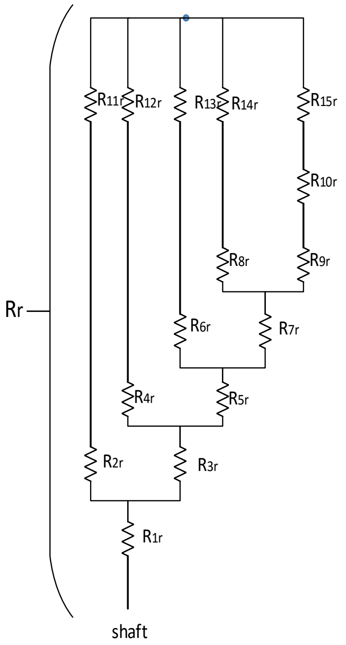

Fig. 4. The thermal equivalent circuit of the rotor.

Figure 4 shows the equivalent thermal circuit for the calculation of the total thermal resistance from the rotor surface to the shaft, which is illustrated by R_r. Furthermore, the value of R_r is equal to the sum of the values of R_{10} and R_{11}. Accordingly, R_r consists of the series-parallel combinations of thermal resistances which the values of thermal resistances R_{11r} to R_{15r} are calculated by (2) and the rest are evaluated by (1). Finally, by using the series-parallel resistances law in the electrical circuit the value of R_r is calculated.

$$R = \frac{l}{\lambda \cdot A}, \tag{1}$$

$$R = \frac{\ln\left(r_o \big/ r_i \right)}{\lambda \cdot L \cdot \phi}, \tag{2}$$

where l is the length of heat flux path (m), A is the cross-section area (m^2), λ is the thermal conductivity of the material (W/m.K), r_o and r_i are the outer radius and the inner radius of cylinder (m), L is the active length of the machine (m) and ϕ is the angular span (rad).

C. Analytical Nodal Temperature Calculation

For the steady-state thermal analysis, the final nodal temperatures of Fig. 2 can be calculated by the matrix inversion theory [12]. Accordingly, the nodal temperatures of the proposed thermal model are calculated as follow:

$$[\mathrm{T}] = [\mathrm{G}]^{-1}[\mathrm{P}], \tag{3}$$

where [T] is the temperature column vector, [P] is the power column vector which contains the losses at each node and [G] is the thermal conductance square matrix which is defined as:

$$\mathbf{G} = \begin{bmatrix} \sum_{i=1}^{n} \frac{1}{R_{1,i}} & \frac{-1}{R_{1,2}} & \cdots & \frac{-1}{R_{1,n}} \\ \frac{-1}{R_{2,1}} & \sum_{i=1}^{n} \frac{1}{R_{2,i}} & \cdots & \frac{-1}{R_{2,n}} \\ \vdots & \vdots & \ddots & \vdots \\ \frac{-1}{R_{n,1}} & \frac{-1}{R_{2,n}} & \cdots & \sum_{i=1}^{n} \frac{1}{R_{n,i}} \end{bmatrix} \tag{4}$$

The $G_{i,i}$ components in the main diagonal of the thermal conductance matrix are defined as the sum of the conductances connected to the i-th node and $G_{i,j}$ is defined as the negative thermal conductances between nodes i and j.

III. EXPERIMENTAL METHODOLOGY

The objective of the experimental work in the natural cooling mode is to determine the value of the natural convection and radiation thermal resistance (R_0) as well as the accuracy of the analytical calculation based on the LPTN model.

According to [9], the value of the resistance R_0 is evaluated by using DC stator test. The DC stator test is a common experimental method for determining the value of the resistance R_0. In this test, the loss of SynRM is confined to the joule loss of the stator coil windings where the electric power can be easily measured. In the calculations, we accounted for the variations in the winding electrical resistance, as the winding resistivity is temperature dependent [12],[13]. During the experiments, the DC power applied to the motor is measured as well as the surface temperature of the motor at different locations. The SynRM is supplied through a digital DC power supply, since the forced cooling air speed is zero and the motor is cooled by natural convection, the motor is supplied with 40% -70% of its nominal current for overheat protection. Four K-type thermocouples are installed by means of adhesive material in various locations on the frame surface of the motor. The ambient temperature is also measured by means of a K-type thermocouple. For the purpose of increasing the accuracy of the temperature measurement and minimizing the contact resistance between the thermocouple and the frame surface of the motor, we used thermal paste. The average temperature of these four thermocouples is assumed to be the mean temperature of the motor frame surface. During the experiments, all the temperature data are collected by means of a Graphtec GL200. The experiment has been carried out until the system reached its steady-state condition. The resistance R_0 is then calculated as [14]:

$$R_0 = \frac{T_s - T_a}{P}, \qquad (5)$$

where T_s is the frame surface temperature (□), T_a is the ambient temperature (□) and P is the input DC power (W).

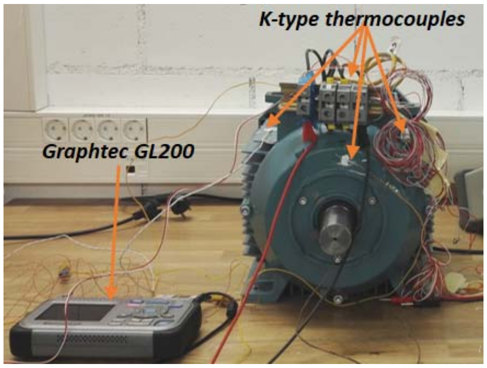

Fig. 5. SynRM test setup.

Figure 5 shows the experimental setup and different location of the surface frame thermocouples. In addition to the surface temperature, the temperature inside the machine was also measured. For this purpose, six different thermocouples have been installed inside the end-windings and slots of the stator. Finally, all measured temperature values are used to validate the developed thermal model.

IV. RESULTS AND DISCUSSION

The DC measurements were carried out at current equals to 40% of the nominal current of the machine, i.e. 8.71 (A). It then took about seven hours to reach the steady-state thermal behavior.

In the steady state mode, the input power was 191.16 (W), the mean temperature of the frame surface was 61.2 (□) and the ambient temperature was 21.8 (□). Finally, the evaluated value of R_0 by using (5) was 0.2056 (□/W).

TABLE IV

Analytical and Experimental Temperature of Motor Components

Machine components	Analytical thermal model	Experimental mean temperature
Frame surface (□)	59.4	61.2
Winding (□)	70.8	74
End winding (□)	76.7	78

To validate the developed thermal model, the analytically calculated temperatures are compared with the experimental data. We present the analytical and experimental results in Table IV. Accordingly, the analytical results are in good agreement with those obtained by the experimental method. The mean difference in the temperature between the analytical and experimental results is around 3%. This difference arises from the hypothesis of the uniform distribution of losses in the machine as well as from the fact that the analytical LPTN model predicts the mean temperature of the machine component while in the experimental part, the thermocouples show the temperatures at given positions. This fact is illustrated in Fig. 6, which shows the temperature distribution over the frame surface of the SynRM in the steady-state mode. The picture is captured by a thermal camera. The figure gives a good overview of the temperature difference on the frame surface of the SynRM. however, The result shows that the presented thermal model can be applied for temperature perdition of the SynRM.

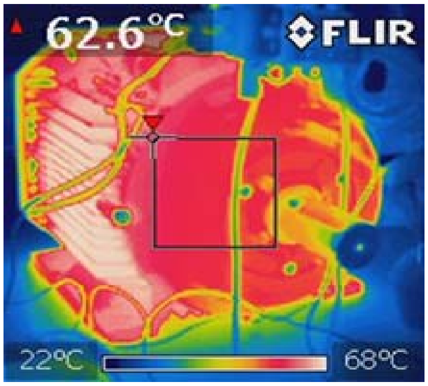

Fig. 6. The surface temperature of SynRM.

V. CONCLUSION

A steady-state LPTN of a transverse-laminated SynRM has been presented. It makes it possible to predict the temperature of the important parts of the machine. We have implemented some simplification hypothesis to reduce the complexity of the model to decrease the computation time without compromising the accuracy of the temperature prediction.

The experimental results of the SynRM under DC stator test have been compared to the LPTN predicted temperatures. The agreement between the analytical temperature and the measured ones seems to be very good. For the future job, the thermal model of the machine will be adjusted to predict the temperature of the machine under forced cooling and normal operation of the machine. For this reason, a radiation thermal resistance and a forced convection thermal resistance parallel to the natural convection one will be in the thermal model.

REFERENCES

[1] A. Boglietti, A. Cavagnino, M. Pastorelli, D. Staton, and A. Vagati, “Thermal analysis of induction and synchronous reluctance motors,” IEEE Trans. Ind. Appl., vol. 42, no. 3, pp. 675–680, May 2006.

[2] P. S. Ghahfarokhi, A. Kallaste, A. Belahcen, T. Vaimann, and A. Rassolkin, “Review of thermal analysis of permanent magnet assisted synchronous reluctance machines,” in 2016 Electric Power Quality and Supply Reliability (PQ), 2016, pp. 219–224.

[3] A. Boglietti, A. Cavagnino, D. Staton, M. Shanel, M. Mueller, and C. Mejuto, “Evolution and Modern Approaches for Thermal Analysis of Electrical Machines,” IEEE Trans. Ind. Electron., vol. 56, no. 3, pp. 871–882, Mar. 2009.

[4] A. Boglietti, A. Cavagnino, and D. Staton, “Determination of Critical Parameters in Electrical Machine Thermal Models,” IEEE Trans. Ind. Appl., vol. 44, no. 4, pp. 1150–1159, 2008.

[5] A. M. EL-Refaie, N. C. Harris, T. M. Jahns, and K. M. Rahman, “Thermal Analysis of Multibarrier Interior PM Synchronous Machine Using Lumped Parameter Model,” IEEE Trans. Energy Convers., vol. 19, no. 2, pp. 303–309, Jun. 2004.

[6] P. H. Mellor, D. Roberts, and D. R. Turner, “Lumped parameter thermal model for electrical machines of TEFC design,” IEE Proc. B Electr. Power Appl., vol. 138, no. 5, p. 205, 1991.

[7] A. Boglietti, A. Cavagnino, M. Popescu, and D. Staton, “Thermal Model and Analysis of Wound-Rotor Induction Machine,” IEEE Trans. Ind. Appl., vol. 49, no. 5, pp. 2078–2085, Sep. 2013.

[8] O. I. Okoro, “Steady and Transient States Thermal Analysis of a 7.5-kW Squirrel-Cage Induction Machine at Rated-Load Operation,” IEEE Trans. Energy Convers., vol. 20, no. 4, pp. 730–736, Dec. 2005.

[9] A. Boglietti, A. Cavagnino, M. Lazzari, and M. Pastorelli, “A simplified thermal model for variable-speed self-cooled industrial induction motor,” IEEE Trans. Ind. Appl., vol. 39, no. 4, pp. 945–952, Jul. 2003.

[10] J. Lindström, “Thermal Model of a Permanent-Magnet Motor for a Hybrid Electric Vehicle,” CHALMERS UNIVERSITY OF TECHNOLOGY, Goteborg, 1999.

[11] M. A. H. Rasid, A. Ospina, K. El Kadri Benkara, and V. Lanfranchi, “Thermal model of stator slot for small synchronous reluctance machine,” in 2014 International Conference on Electrical Machines (ICEM), 2014, pp. 2199–2204.

[12] P. S. Ghahfarokhi, A. Kallaste, A. Belahcen, and T. Vaimann, “Steady state and transient thermal analysis of the stator coil of a permanent magnet generator,” in 2017 18th International Scientific Conference on Electric Power Engineering (EPE), 2017, pp. 1–5.

[13] P. S. Ghahfarokhi, A. Kallaste, A. Belahcen, T. Vaimann, “Determination of Forced Convection Coefficient Over a Flat Side of Coil,” in 58th International Scientific Conference on Power and Electrical Engineering of Riga Technical University (RTUCON), 2017, pp. 1–4.

[14] A. Boglietti, A. Cavagnino, and D. A. Staton, “Thermal analysis of TEFC induction motors,” in 38th IAS Annual Meeting on Conference Record of the Industry Applications Conference, 2003., vol. 2, pp. 849–856.

BIOGRAPHIES

Payam Shams Ghahfarokhi was born in Iran, in 1986. He received the B.Sc. degree in electrical power engineering from IAUN in 2010 and the M.Sc. degree in electrical power engineering from Newcastle University in 2011. He is currently a Ph.D. student at Tallinn University of Technology. He has been the student IEEE member since 2017. His main field of interests is design of permanent magnet electrical machine and thermal design of electrical machine.

Anouar Belahcen (M13-SM15) received the M.Sc. (Tech.) and Doctor (Tech.) degrees from Helsinki University of Technology, Finland, in 1998, and 2004, respectively. He is now Professor of electrical machines at Tallinn University of Technology, Estonia and Professor of Energy and Power at Aalto University, Finland. His research interest are numerical modeling of electrical machines, magnetic materials, coupled magneto-mechanical problems, magnetic forces, magnetostriction, and fault diagnostics

Ants Kallaste was born in Pärnu, Estonia in 1980 and received his B.Sc., M.Sc., and Ph.D. degrees in electrical engineering from Tallinn University of Technology, Estonia, in 2004, 2006, and 2013, respectively. He is currently a Senior Researcher in Tallinn University of Technology, Department of Electrical Engineering and carrying out postdoctoral research at the Department of Electrical Engineering and Automation, Aalto University, Espoo, Finland. He has been working in several companies as an Electrical Engineer. Presently he is working at the Tallinn University of Technology, Department of Electrical Engineering holding the position of Head of Chair of Electrical Machines. He has been the IEEE member since 2013. His main research interests include permanent magnet machine design and wind turbines.

Toomas Vaimann (S'11-M'14)was born in Pärnu, Estonia, in 1984 and received his B.Sc., M.Sc., and Ph.D. degrees in electrical engineering from Tallinn University of Technology, Estonia, in 2007, 2009. and 2014, respectively. He is currently a Senior Researcher in Tallinn University of Technology, Department of Electrical Engineering and carrying out postdoctoral research at the Department of Electrical Engineering and Automation, Aalto University, Espoo, Finland. He has been working in several companies as an Electrical Engineer. He is the member of IEEE, Estonian Society of Moritz Hermann Jacobi and Estonian Society for Electrical Power Engineering. His main research interest is the diagnostics of electrical machines.

Anton Rassõlkin (S'12-M'16). was born in Tallinn, Estonia, in 1985 and received the BSc, MSc and PhD degrees in electric drives and power electronics from Tallinn University of Technology, Tallinn, Estonia, in 2008, 2010 and 2014, respectively. In 2010 received Dipl.-Ing. (FH) degree in automatic from University of Applied Science Giessen-Friedberg, Giessen, Germany. He has been working in several companies as an electrical engineer. Presently he is working at the Tallinn University of Technology, Department of Electrical Engineering as a research scientist. He is the member of IEEE The main research interests lay in the field of electric drives and its control systems as well as in the fields of electrical machines and electric transportation.

.